ELSEVIER

Journal of Photochemistry and Photobiology A: Chemistry 99 (1996) 177–183

Journal of PHOTOCHEMISTRY AND PHOTOBIOLOGY A: CHEMISTRY

The effect of methylviologen on the photoluminescence bands of quantum-sized CdS

M. Hamity *, R.H. Lema

Departamento de Química y Física, Universidad Nacional de Río Cuarto, 5800 Río Cuarto (Córdoba), Argentina

Received 26 February 1996; accepted 9 May 1996

Abstract

Colloidal, quantum-sized CdS (Q-CdS) particles displaying an isolated fluorescence band, with a maximum fluorescence wavelength at 487, 580 or 709 nm, were prepared. From the excitation spectra, the onset of the bands was determined, giving the band gaps of the clusters as 2.88, 2.71 and 2.54 eV respectively. The effect of methylviologen dication (Mv^{2+}) on the fluorescence quantum yield and lifetime of the colloidal Q-CdS particles was studied. With the experimental data obtained, an equilibrium constant for the formation of adducts between Mv^{2+} and Q-CdS particles was evaluated. Partial quenching of the fluorescence at 487 nm, nearly complete quenching of the fluorescence at 580 nm and total quenching of the 709 nm band were attained. The quenching was dynamic or a combination of static and dynamic, depending on the energy of the emission. Static quenching was only observed for the clusters emitting a fluorescence band with a maximum at 709 nm. For the fluorescence bands with maxima at 487 and 580 nm, it was only possible to observe dynamic quenching. A mechanistic scheme which accounts for the experimental results is given for each cluster system. Within the proposed schemes, radiative processes do not arise from the trapped electrons. Instead, they originate from the interaction between conduction electrons or detrapped electrons and deep trapped holes.

Keywords: Methylviologen; Photoluminescence; Quantum-sized CdS

1. Introduction

The photochemistry and photophysics of colloidal semiconductor particles are currently the subject of a large number of research publications [1,2]. Of great interest to research workers are the size quantization effects and unusual fluorescence behaviour observed for these colloidal particles in the nanometre size range [3–6].

In bulk semiconductor material, an electron–hole pair is formed by the absorption of a photon; this electron–hole pair may exist as a Wannier exciton or as a free charge carrier in the conduction and valence band. The fluorescence spectrum normally shows a sharp band located near the onset of absorption (attributed to the recombination of free charge carriers and assigned as excitonic fluorescence) and a broad, red-shifted band (due to the recombination of charge carriers trapped at different sites of the crystal and assigned as trapped fluorescence). In the latter case, the electrons must move via the conduction band after being detrapped, or may tunnel to a positive trap [7].

The fluorescence properties (spectral position, ratio of excitonic to trapped fluorescence and absolute intensity) of quantum confined semiconductor (Q-SC) particles are influenced by temperature changes [7], surface modifications [8] and particle size [9,10].

Fluorescence investigations are a convenient method to obtain information on the energetics and dynamics of photogenerated charge carriers in small particles. Chandler and Coffer [11] have studied the effect of several stabilizers on the fluorescence behaviour of quantum-sized CdS (Q-CdS) particles in inverse micelles and several organic solvents. They obtained partial quenching of the trapped fluorescence of the Q-CdS clusters with methylviologen and halide ions. Hässelbarth et al. [12] have carried out stationary and time-resolved quenching of the excitonic and trapped fluorescence of Q-CdS colloids with nitromethane and methylviologen. They concluded that the quenching of the excitonic fluorescence was mainly dynamic, whereas the quenching of the trapped fluorescence was both dynamic and static. The samples investigated showed both excitonic and trapped fluorescence bands.

We have prepared Q-CdS samples which exhibit an isolated, either excitonic or trapped, fluorescence band. This allows the effect produced by several quenchers on individual bands to be studied separately and enables new experimental evidence to be obtained on the characteristics of the surface

* Corresponding author.

PII S1010-6030(96)04403-6

of the clusters. In this paper, we report the effect produced by the methylviologen dication (Mv^{2+}) on these individual bands. A mechanistic scheme which accounts for the experimental results obtained is given for each cluster system.

2. Experimental details

2.1. Chemicals

Sodium polyphosphate (Merck, extra pure), sodium sulphide (Merck, p.a.), cadmium sulphate (Mallinckrodt, p.a.) and methylviologen dichloride (Sigma) were used without further purification.

2.2. Preparation of Q-CdS colloids

2.2.1. Excitonic fluorescence band

Samples with only one band with a maximum emission wavelength at 487 nm were prepared, according to Spanhel et al. [9], by adding H_2S to an aqueous solution of $CdSO_4$ (2×10^{-4} M) containing sodium polyphosphate (2×10^{-4} M) as stabilizer until a pale yellow colour was obtained. The solution was previously degassed with argon and its pH was adjusted to pH 9. The fluorescence was then activated by adding $CdSO_4$ to obtain a final concentration of 8×10^{-4} M, and the pH was finally adjusted to pH 10.5 with NaOH.

2.2.2. Trapped fluorescence bands

Clusters with a maximum emission at 580 nm were prepared similarly to the excitonic band samples, except that the starting pH was adjusted to pH 10, the initial ratio of Cd^{2+} to polyphosphate was 1 : 2 and the $CdSO_4$ final concentration was 4×10^{-4} M. Alternatively, this fluorescence band was obtained by the dropwise addition of an Na_2S solution, instead of H_2S, to a Cd^{2+}–polyphosphate solution until no increment in the emission intensity was observed. The $[Cd^{2+}]/[(NaPO_3)_6]/[S^{2-}]$ final ratio was 4 : 4 : 1.

The samples with a fluorescence band with a maximum at 709 nm were prepared by the slow addition of an Na_2S solution to a previously degassed aqueous solution of $CdSO_4$ (2×10^{-4} M) and sodium polyphosphate (2×10^{-4} M) at pH 7, until no increment in the emission intensity was observed. No activation with $CdSO_4$ was carried out. The $[Cd^{2+}]/[(NaPO_3)_6]/[S^{2-}]$ final ratio was 2 : 2 : 1. The pH was finally adjusted to pH 10 with NaOH solution.

2.3. Quenching procedures

The quenching experiments with several samples showing isolated fluorescence bands were carried out by adding a concentrated Mv^{2+} solution to the corresponding Q-CdS solution, so as to make dilution effects negligible. Both quencher and Q-CdS solutions were deoxygenated by nitrogen bubbling to prevent photo-anodic corrosion [13], and the pH was kept constant at a value of pH 9 during all the experiments.

The fluorescence quantum yields were determined with the reference standards quinine sulphate for the 487 nm band and tris-(2,2′-bipyridine)ruthenium(II) for the trapped fluorescence bands.

2.4. Apparatus

UV–visible absorption measurements were performed with a Hewlett Packard HP 8452 A diode array spectrophotometer.

Fluorescence spectra were taken with a Spex FluoroMax™ spectrofluorometer.

Fluorescence decay profiles were registered by employing a fluorescence lifetime equipment consisting of a Laseroptics nitrogen laser (5 ns FWHM) as the excitation source. The sample was located in the cavity of a TRW 75-A filter fluorometer. The different fluorescence bands were isolated by a suitable combination of band and cut-off filters. The signal of the photomultiplier was displayed, averaged and digitized by a Hewlett Packard 54200 A oscilloscope. It was then transferred via an IEEE interface to an IBM-AT computer, where it was processed.

3. Results and discussion

As described in Section 2, we were able to obtain samples that displayed only one fluorescence band. These bands present emission maxima at 487 nm (excitonic), 580 nm and 709 nm (trapped fluorescence), as shown in Fig. 1. From the onset of the excitation spectra, we obtained the different band gaps for each of the clusters: 2.88, 2.7 and 2.54 eV respectively. It is important to note that the positions of the different emission bands do not depend on the excitation wavelength. This may indicate that the sizes of the particles present in each of the clusters are approximately homogeneous. The fluorescence quantum yields (ϕ_f) determined for these bands

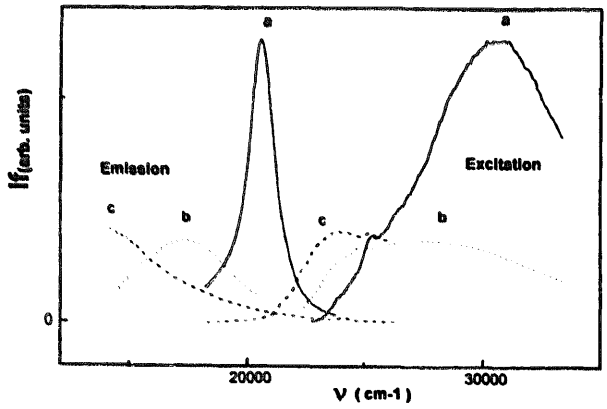

Fig. 1. Fluorescence excitation and emission spectra of the clusters: (a) excitonic band (λ_{max} = 487 nm); (b) trapped fluorescence band (λ_{max} = 580 nm); (c) trapped fluorescence band (λ_{max} = 709 nm). All spectra were monitored at maximum intensity.

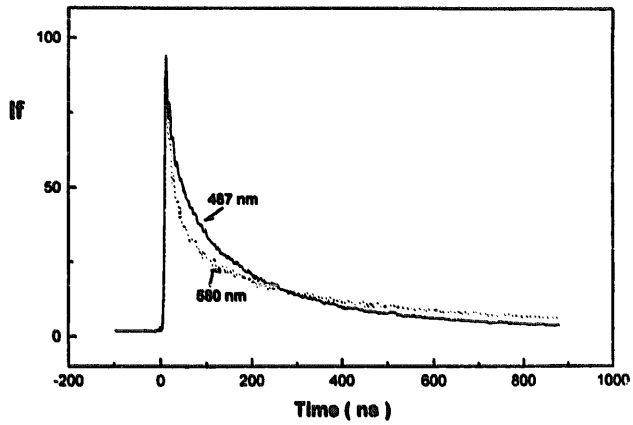

Fig. 2. Fluorescence decay profiles for clusters emitting an excitonic band (λ_{max} = 487 nm) and one trapped fluorescence band (λ_{max} = 580 nm).

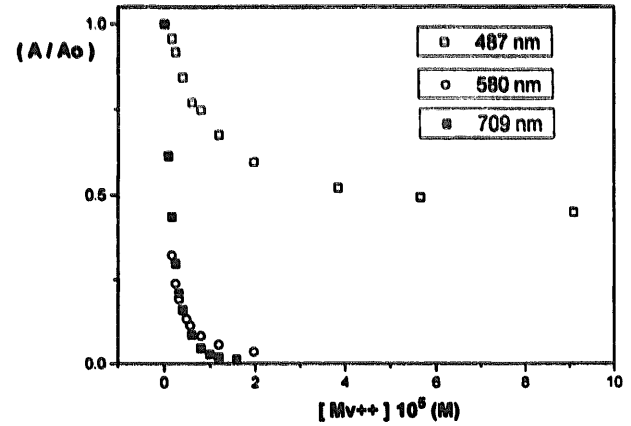

Fig. 3. Relative fluorescence emission intensity, expressed as the peak area (A/A_0), as a function of the added methylviologen concentration for clusters emitting at maximum wavelengths of 487 nm (□), 580 nm (○) and 709 nm (▽).

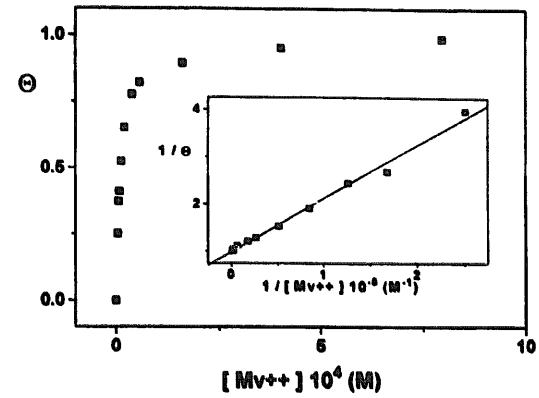

Fig. 4. Langmuir adsorption isotherm plot for CdS samples emitting the excitonic band (λ_{max} = 487 nm). Inset: double reciprocal plot of $1/\Theta$ vs. $1/[Mv^{2+}]$.

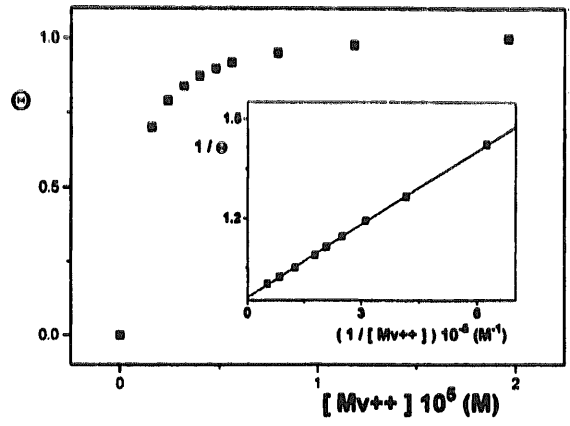

Fig. 5. Langmuir adsorption isotherm plot for samples emitting one trapped fluorescence band (λ_{max} = 580 nm). Inset: double reciprocal plot of $1/\Theta$ vs. $1/[Mv^{2+}]$.

were similar (0.1). We also determined the fluorescence decay profiles for the 487 and 580 nm bands and found that each of the bands shows a non-exponential decay (Fig. 2).

We also studied the effect of Mv^{2+} on the fluorescence of the different bands of Q-CdS in the absence of oxygen. We observed a quenching of the fluorescence as shown in Fig. 3.

If the change in the photoluminescence intensity is attributed to the formation of an adduct between the quencher and the colloidal particles, an equilibrium constant (K) can be calculated [14]. The fractional change in the peak area (Θ) represents the fraction of surface sites occupied by the quencher

$$\Theta = \frac{\Delta F}{|F_{sat} - F_0|} = \frac{K[Q]}{1 + K[Q]}$$

where F_0 is the fluorescence intensity in the absence of quencher Q, $\Delta F = |F_{sat} - F_0|$ is the fluorescence intensity change after each quencher addition to obtain a quencher concentration [Q] and F_{sat} is the fluorescence intensity at saturation, corresponding to the maximum occupation of the surface by the quencher. An alternative method for the measurement of ΔF employed the values of the peak area and fluorescence intensity at the maximum wavelength, and similar results were obtained.

A plot of Θ vs. [Q] yields a Langmuir-type adsorption isotherm. The Langmuir plot obtained for the samples emitting at 487 nm is shown in Fig. 4 and that for the 580 nm band clusters is shown in Fig. 5. From the slopes of the double reciprocal plots of $1/\Theta$ vs. $1/[Q]$, shown as insets in Figs. 4 and 5, the values of the equilibrium constants for adduct formation were obtained as 1×10^5 and 1.3×10^6 respectively. The double reciprocal plot for the 709 nm band is not linear, which may indicate the occurrence of more than one quenching process.

According to the values of the equilibrium constant for adduct formation obtained, we believe that Mv^{2+} is almost completely adherent to the colloid surface, i.e. the concentration of methylviologen adherent to the surface is nearly equal to the analytical concentration.

3.1. Quenching of excitonic fluorescence

The effect of adding Mv^{2+} to a solution of Q-CdS exhibiting a fluorescence band with a maximum at 487 nm is shown in Fig. 3. A partial quenching effect is obtained in this case.

This fluorescence is generally attributed to electrons emitting from the conduction band [2,7,12]. However, we believe that a distinction must be made between prompt fluorescence, due to electrons excited to and emitting directly from the conduction band, and delayed fluorescence, whereby electrons which are in very shallow surface traps emit from the conduction band after being detrapped. In order to explain the partial quenching shown in Fig. 3, we assume that Mv^{2+} can interact with the trapped electrons, but not with those emitting directly from the conduction band.

A plausible mechanistic scheme which can account for the observed experimental facts is given below

$$Q_{solution} \leftrightarrow Q_{adherent} \quad (1)$$

$$CdS + h\nu \rightarrow (h^+; e^-) \quad (2)$$

$$(h^+; e^-) \rightarrow CdS \quad (3)$$

$$(h^+; e^-) \rightarrow h^+_{surf.} + e^-_{surf.} \quad (4)$$

The surface hole is located in deep traps (h^+_T), while surface electrons are in the conduction band (e^-_C) and can be trapped in very shallow traps (T1)

$$e^-_C \rightarrow e^-_{T1} \quad (5)$$

The electrons in traps (e^-_{T1}) can return to the conduction band $(e^-_C)_D$ as follows

$$e^-_{T1} \rightarrow (e^-_C)_D \quad (6)$$

The non-radiative processes can be represented as

$$e^-_C + h^+_T \rightarrow CdS \quad (7)$$

$$(e^-_C)_D + h^+_T \rightarrow CdS \quad (8)$$

$$e^-_{T1} + h^+_T \rightarrow CdS \quad (9)$$

While the radiative processes are

$$e^-_C + h^+_T \rightarrow h\nu' \text{ (prompt fluorescence)} \quad (10)$$

$$(e^-_C)_D + h^+_T \rightarrow h\nu' \text{ (delayed fluorescence)} \quad (11)$$

The fluorescence quenching step is

$$e^-_{T1} + Q_{ad} \rightarrow \text{quenching} \quad (12)$$

The residual fluorescence that can be seen in Fig. 3 is the prompt fluorescence (Eq. (10)). The trapping of conduction band electrons on the particle surface (Eq. (5)) occurs in a period of time of less than 1 ps [15]. Therefore the lifetime of electrons in the conduction band (e^-_C) must be of the order of picoseconds so that Eq. (10) can compete with Eq. (5), and so that the Mv^{2+} adherent to the surface cannot interact with them to quench the prompt fluorescence.

According to the mechanistic scheme presented above, the total fluorescence in the absence of quencher (F^0_T), arising from Eqs. (10) and (11), can be expressed as

$$F^0_T = F^0_{10} + F^0_{11} \quad (13)$$

When a quencher (Q) is added, assuming that F^0_{11} decreases following the Stern–Volmer equation, while the rest of the fluorescence (F^0_{10}) is not affected, the total fluorescence in the presence of quencher is given by

$$F_T = \frac{F^0_{11}}{1 + K_{SV}[Q]} + F^0_{10} \quad (14)$$

Subtracting Eq. (14) from Eq. (13), dividing by F^0_T and taking the reciprocal, we obtain

$$\frac{F^0_T}{\Delta F_T} = \frac{1}{f_{11} K_{SV}[Q]} + \frac{1}{f_{11}} \quad (15)$$

where K_{SV} is the Stern–Volmer constant for the quenching of the delayed fluorescence and f_{11} represents the fraction of total fluorescence that can be quenched ($f_{11} = F^0_{11}/F^0_T$). From the mechanistic scheme given above, assuming steady state for the involved transients, the Stern–Volmer constant can be expressed as $K_{SV} = k_{12}\tau_{eT1}$. In this expression, k_{12} is the rate constant for the quenching process (k_Q) and τ_{eT1} represents the average residence time of the electrons in the traps T1 ($\tau_{eT1} = 1/(k_6 + k_9[h^+_T])$).

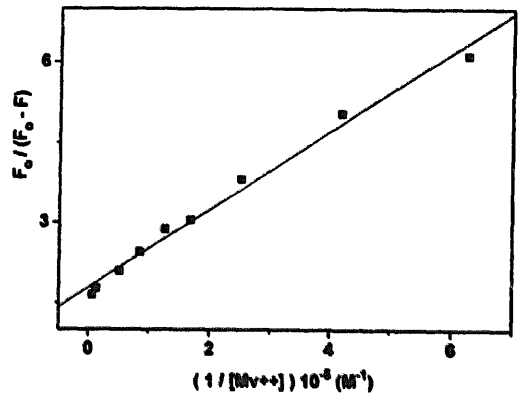

Fig. 6. Emission fluorescence intensity data for the excitonic band, plotted in the form of Eq. (15).

A plot of the left part of Eq. (15) as a function of the inverse Mv^{2+} concentration is shown in Fig. 6. From the intercept of this plot, a value of $f_{11} = 0.56$ is obtained, which indicates that 56% of the fluorescence arises from detrapped electrons $(e^-_C)_D$ and 44% arises from electrons in the conduction band which have not been trapped. From the slope of this plot, a value of $K_{SV} = 2.4 \times 10^5\ M^{-1}$ is obtained for the Stern–Volmer constant.

The fluorescence decay curves after the addition of different amounts of Mv^{2+} are shown in Fig. 7. The initial signal height is nearly the same for all $[Mv^{2+}]$. This indicates that the quenching process is mainly dynamic on the surface.

3.2. *Quenching of trapped fluorescence*

3.2.1. *Band with maximum emission wavelength at 709 nm*

The effect of adding Mv^{2+} to a solution of Q-CdS exhibiting a fluorescence band with a maximum at 709 nm is shown in Fig. 3. In this case, we obtain total fluorescence quenching. The Stern–Volmer plot does not show a linear behaviour, as can be seen in Fig. 8. These results can be explained in accord with the mechanistic scheme given below.

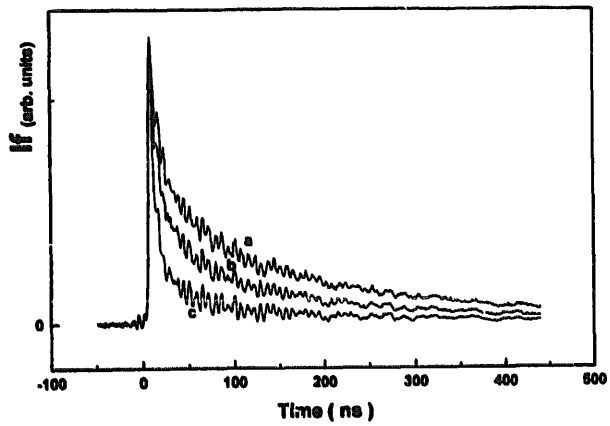

Fig. 7. Fluorescence decay profiles for clusters emitting excitonic fluorescence for several concentrations of methylviologen added. [Mv^{2+}]: (a) 0 M; (b) 4×10^{-6} M; (c) 1.6×10^{-5} M.

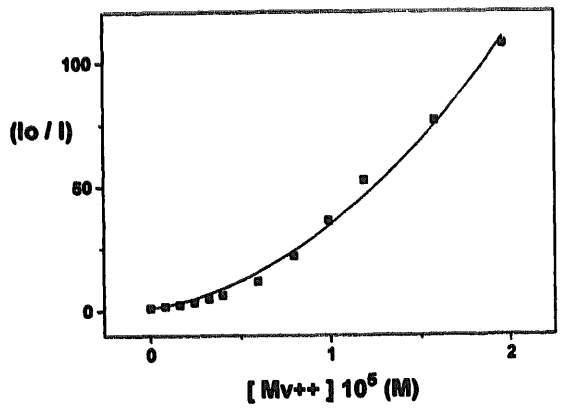

Fig. 8. Stern–Volmer plot for the experimental data of the trapped fluorescence band with $\lambda_{max}=709$ nm (■). Full line shows the fitting of the fluorescence emission data for the band with $\lambda_{max}=709$ nm to the quadratic expression given by Eq. (24).

The four initial steps are similar to Eqs. (1)–(4) of the scheme shown above for the 487 nm band, except that (h^+; e^-) may decay to deep traps, symbolized as $h^+{}_T$ and $e^-{}_{T3}$ respectively

$$Q_{solution} \leftrightarrow Q_{adherent}$$

$$CdS + h\nu \rightarrow (h^+; e^-)$$

$$(h^+; e^-) \rightarrow CdS$$

$$(h^+; e^-) \rightarrow h_T^+ + e_{T3}^- \quad (16)$$

The electrons $e^-{}_{T3}$ can move to traps of nearly the same energy level, as mobile electrons $e^-{}_{M3}$. However, since the excitonic fluorescence is not observed from these clusters, they cannot reach the conduction band

$$e_{T3}^- \rightarrow e_{M3}^- \quad (17)$$

The non-radiative processes are

$$e_{T3}^- + h_T^+ \rightarrow CdS \quad (18)$$

$$e_{M3}^- + h_T^+ \rightarrow CdS \quad (19)$$

While the radiative process is

$$e_{M3}^- + h_T^+ \rightarrow h\nu' \quad (20)$$

The fact that the Stern–Volmer plot is non-linear indicates that both dynamic and static quenching processes occur simultaneously.

We consider that dynamic quenching occurs when a trapped electron moves to another trap already occupied by Mv^{2+}

$$e_{T3}^- + Q_{ad} \rightarrow (\text{dynamic quenching}) \quad (21)$$

Static quenching occurs when an electron enters a trap where Mv^{2+} is adsorbed

$$(h^+; e^-) + Q_{ad} \rightarrow e_{T3,Q}^- \text{ (static quenching)} \quad (22)$$

This step competes with the electron trapping step (Eq. (16)).

According to the mechanistic scheme presented above, the fluorescence intensity is given through Eq. (20) as

$$I_f = k_{20}(e_{M3}^-)(h_T^+) \quad (23)$$

Assuming steady state for the transients ($e^-{}_{M3}$, $e^-{}_{T3}$, $h^+{}_T$ and (h^+; e^-)), we obtain for the ratio of the quantum yields in the absence and presence of quencher

$$\frac{\phi^0}{\phi} = 1 + (P_1 + P_2)[Q] + P_1P_2[Q]^2 \quad (24)$$

where

$$P_1 = \frac{k_{21}}{(k_{17} + k_{18}[h_T^+])} \text{ and } P_2 = \frac{k_{22}}{(k_3 + k_{16})}$$

The parameters P_1 and P_2 represent the Stern–Volmer constants (K_{SV}) for dynamic and static quenching respectively, where k_{21} and k_{22} are the quenching constants (k_Q) and

$$\tau_{T3}^0 = \frac{1}{(k_{17} + k_{18}[h_T^+])} \text{ and } \tau_E^0 = \frac{1}{(k_3 + k_{16})}$$

are the average residence time of the electrons in the traps T3 and the lifetime of the exciton (h^+; e^-) respectively. In Fig. 8, the full line represents the fitting of the quadratic expression (Eq. (24)) to the experimental data. The values obtained for the parameters are $P_1 = 7.8\times10^5$ M^{-1} and $P_2 = 2.9\times10^5$ M^{-1}.

3.2.2. *Band with maximum emission wavelength at 580 nm*

The effect of adding Mv^{2+} to a solution of Q-CdS exhibiting a fluorescence band with a maximum at 580 nm is also shown in Fig. 3. In this case, we obtain nearly complete fluorescence quenching with a linear Stern–Volmer plot, which is shown in Fig. 9.

These results can be explained by a mechanistic scheme similar to that presented for the 709 nm band, except that the electron traps (T2) are shallower than T3 and the trapped electrons are represented as $e^-{}_{T2}$. The experimental data can be explained assuming that there is only one quenching process. We believe that this is a dynamic process, since the initial

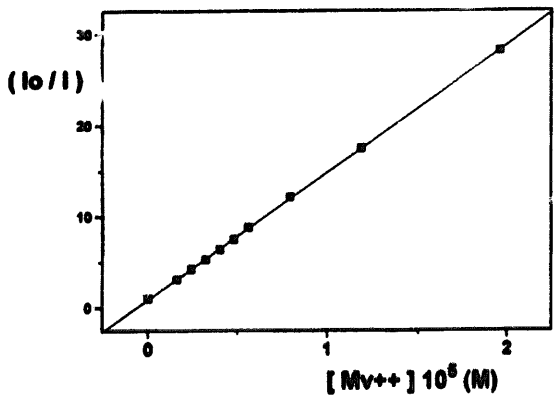

Fig. 9. Stern–Volmer plot for the trapped fluorescence band with $\lambda_{max} = 580$ nm.

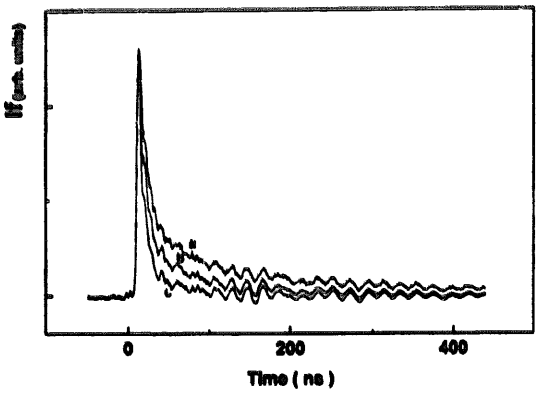

Fig. 10. Fluorescence decay profiles for clusters emitting trapped fluorescence with $\lambda_{max} = 580$ nm for several concentrations of methylviologen added. [Mv^{2+}]: (a) 0 M; (b) 4×10^{-6} M; (c) 1.6×10^{-5} M.

signal height for the fluorescence decay curve after the addition of Mv^{2+} is nearly constant, as shown in Fig. 10.

The mechanistic scheme is as follows

$$Q_{solution} \leftrightarrow Q_{adherent}$$

$$CdS + h\nu \rightarrow (h^+, e^-)$$

$$(h^+; e^-) \rightarrow CdS$$

$$(h^+; e^-) \rightarrow h_T^+ + e_{T2}^- \quad (25)$$

$$e_{T2}^- \rightarrow e_{M2}^- \quad (26)$$

The non-radiative processes are

$$e_{T2}^- + h_T^+ \rightarrow CdS \quad (27)$$

$$e_{M2}^- + h_T^+ \rightarrow CdS \quad (28)$$

While the radiative process is

$$e_{M2}^- + h_T^+ \rightarrow h\nu'' \quad (29)$$

The quenching process is

$$e_{T2}^- + Q_{ad} \rightarrow \text{dynamic quenching} \quad (30)$$

Since static quenching is not observed for these clusters, the traps (T2) are not occupied by the quencher. According to this mechanistic scheme, the fluorescence intensity is given through Eq. (29) as

$$I_f = k_{29}(e_{M2}^-)(h_T^+) \quad (31)$$

Assuming steady state for the transients (e^-_{M2}, e^-_{T2}, h^+_T and $(h^+; e^-)$), we obtain for the ratio of the quantum yields in the absence and presence of quencher

$$\frac{\phi^0}{\phi} = 1 + c[Q] \quad (32)$$

where

$$c = \frac{k_{30}}{(k_{26} + k_{27}[h_T^+])}$$

Eq. (32) is a typical Stern–Volmer expression, where c represents the Stern–Volmer constant (K_{SV}), k_{30} is the quenching constant (k_Q) and

$$\tau_{T2} = \frac{1}{(k_{26} + k_{27}[h_T^+])}$$

represents the average residence time of the electrons in the traps T2.

The fitting of the experimental data for clusters emitting at $\lambda_{max} = 580$ nm to Eq. (32) is shown in Fig. 9. From the slope, we obtained the Stern–Volmer constant $K_{SV} = 1.3 \times 10^6 M^{-1}$. This value is close to that obtained for the dynamic quenching constant for the 709 nm band, P_1.

4. Conclusions

We believe that the mechanistic schemes given here are representative of the processes involved in the quenching of the isolated fluorescence bands emitted by the clusters, and that they account for the experimental results. Within the proposed schemes, the radiative processes do not arise from the trapped electrons. Instead, they originate from the interaction between conduction electrons (e^-_C) or detrapped electrons (e^-_D or e^-_M) and deep trapped holes. We consider that, at least under our experimental conditions, tunnelling is not a probable pathway to fluorescence.

The values obtained for the Stern–Volmer constants P_1 (709 nm band) and c (580 nm band) are close to each other. This indicates that the dynamic quenching processes for the trapped fluorescence bands (580 and 709 nm) may be similar. Since the mean lifetimes for both bands are also similar, this implies similar kinetics for the electron detrapping processes (Eqs. (21) and (30) in the mechanisms).

Static quenching is only observed for clusters emitting a fluorescence band with a maximum at 709 nm, in which case the clusters were not activated by adding Cd^{2+}. Therefore, in these clusters, the lack of Cd^{2+} ions on the surface may facilitate the access of Mv^{2+} ions to the surface traps (T3), thus making it possible to observe a static quenching effect. For the fluorescence bands with maxima at 487 nm and 580 nm, the excess of cadmium ions, added to obtain activation of the clusters, may make it difficult for Mv^{2+} ions to reach

the surface traps (T1 and T2), and only dynamic quenching is observed.

Acknowledgements

Thanks are due to the Universidad Nacional de Río Cuarto and CONICOR (Provincia de Córdoba) for financial support. We wish to express our thanks to Dr. C.M. Previtali for valuable discussions and C.A. Suchetti who contributed to the experimental work.

References

[1] A. Hagfeldt and M. Grätzel, *Chem. Rev.*, *95* (1995) 49.
[2] Y. Wang, *Adv. Photochem.*, *19* (1995) 179.
[3] A. Henglein, *Chem. Rev.*, *89* (1989) 1861.
[4] A.D. Yoffe, *Adv. Phys.*, *42* (1993) 173.
[5] H. Weller, *Angew. Chem. Int. Ed. Engl.*, *32* (1993) 41.
[6] L.E. Brus, in G.C. Hadjipanayis and R.W. Siegel (eds.), *Nanophase Materials*, Kluwer, Dordrecht, 1994, p. 433.
[7] A. Eychmüller, A. Hässelbarth, L. Katsikas and H. Weller, *Ber. Bunsenges. Phys. Chem.*, *95* (1991) 79.
[8] P.V. Kamat, M. deLind van Wijngaarden and S. Hotchandani, *Isr. J. Chem.*, *33* (1993) 47.
[9] L. Spanhel, M. Haase, H. Weller and A. Henglein, *J. Am. Chem. Soc.*, *109* (1987) 5649.
[10] L. Spanhel, H. Weller, A. Fojtik and A. Henglein, *Ber. Bunsenges. Phys. Chem.*, *91* (1987) 88.
[11] R.R. Chandler and J.L. Coffer, *J. Phys. Chem.*, *97* (1993) 9767.
[12] A. Hässelbarth, A. Eychmüller and H. Weller, *Chem. Phys. Lett.*, *203* (1993) 271.
[13] A. Henglein, in H.-F. Eicke (ed.), *Modern Trends of Colloid Science in Chemistry and Biology*, Birkhäuser Verlag, 1985, p. 126.
[14] R.R. Chandler and J.L. Coffer, *J. Phys. Chem.*, *96* (1992) 2713.
[15] J.Z. Zhang, R.H. O'Neil and T.W. Roberti, *J. Phys. Chem.*, *98* (1994) 3859.